Nitrate removal in stream ecosystems measured by ^{15}N addition experiments: Total uptake

Robert O. Hall, Jr.,[a,*] Jennifer L. Tank,[b] Daniel J. Sobota,[c,1] Patrick J. Mulholland,[d,e] Jonathan M. O'Brien,[f,g] Walter K. Dodds,[f] Jackson R. Webster,[h] H. Maurice Valett,[h] Geoffrey C. Poole,[i,j] Bruce J. Peterson,[k] Judy L. Meyer,[j] William H. McDowell,[l] Sherri L. Johnson,[m] Stephen K. Hamilton,[g] Nancy B. Grimm,[n] Stanley V. Gregory,[c] Clifford N. Dahm,[o] Lee W. Cooper,[e,2] Linda R. Ashkenas,[c] Suzanne M. Thomas,[j] Richard W. Sheibley,[n,3] Jody D. Potter,[l] B. R. Niederlehner,[h] Laura T. Johnson,[b] Ashley M. Helton,[k] Chelsea M. Crenshaw,[o,4] Amy J. Burgin,[g,5] Melody J. Bernot,[p] Jake J. Beaulieu,[b,6] and Clay P. Arango[b,7]

[a] Department of Zoology and Physiology, University of Wyoming, Laramie, Wyoming
[b] Department of Biological Sciences, University of Notre Dame, Notre Dame, Indiana
[c] Department of Fisheries and Wildlife, Oregon State University, Corvallis, Oregon
[d] Environmental Sciences Division, Oak Ridge National Laboratory, Oak Ridge, Tennessee
[e] Department of Ecology and Evolutionary Biology, University of Tennessee, Knoxville, Tennessee
[f] Division of Biology, Kansas State University, Manhattan, Kansas
[g] Kellogg Biological Station, Michigan State University, Hickory Corners, Michigan
[h] Department of Biological Sciences, Virginia Polytechnic Institute and State University, Blacksburg, Virginia
[i] Department of Land Resources and Environmental Sciences, Montana State University, Bozeman, Montana
[j] Odum School of Ecology, University of Georgia, Athens, Georgia
[k] Ecosystems Center, Marine Biological Laboratory, Woods Hole, Massachusetts
[l] Department of Natural Resources, University of New Hampshire, Durham, New Hampshire
[m] Pacific NW Research Station, U.S. Forest Service, Corvallis, Oregon
[n] School of Life Sciences, Arizona State University, Tempe, Arizona
[o] Department of Biology, University of New Mexico, Albuquerque, New Mexico
[p] Department of Biology, Ball State University, Muncie, Indiana

Abstract

We measured uptake length of $^{15}NO_3^-$ in 72 streams in eight regions across the United States and Puerto Rico to develop quantitative predictive models on controls of NO_3^- uptake length. As part of the Lotic Intersite Nitrogen eXperiment II project, we chose nine streams in each region corresponding to natural (reference), suburban–urban, and agricultural land uses. Study streams spanned a range of human land use to maximize variation in NO_3^- concentration, geomorphology, and metabolism. We tested a causal model predicting controls on NO_3^- uptake length using structural equation modeling. The model included concomitant measurements of ecosystem metabolism, hydraulic parameters, and nitrogen concentration. We compared this structural equation model to multiple regression models which included additional biotic, catchment, and riparian variables. The structural equation model explained 79% of the variation in log uptake length (S_{Wtot}). Uptake length increased with specific discharge (Q/w) and increasing NO_3^- concentrations, showing a loss in removal efficiency in streams with high NO_3^- concentration. Uptake lengths shortened with increasing gross primary production, suggesting autotrophic assimilation dominated NO_3^- removal. The fraction of catchment area as agriculture and suburban–urban land use weakly predicted NO_3^- uptake in bivariate regression, and did improve prediction in a set of multiple regression models. Adding land use to the structural equation model showed that land use indirectly affected NO_3^- uptake lengths via directly increasing both gross primary production and NO_3^- concentration. Gross primary production shortened S_{Wtot}, while increasing NO_3^- lengthened S_{Wtot} resulting in no net effect of land use on NO_3^- removal.

* Corresponding author: bhall@uwyo.edu

Present addresses:
[1] School of Earth and Environmental Sciences, Washington State University, Vancouver Campus, Vancouver, Washington
[2] Chesapeake Biological Laboratory, University of Maryland Center for Environmental Science, Solomons, Maryland
[3] USGS Washington Water Science Center, Tacoma, Washington
[4] Department of Biology, Utah State University, Logan, Utah
[5] Cary Institute of Ecosystem Studies, Box AB, Millbrook, New York
[6] US Environmental Protection Agency, Cincinnati, Ohio
[7] Department of Geography, Central Washington University, Ellensburg, Washington

Humans have doubled the input of nitrogen (N) into the biosphere, fundamentally altering productivity and community structure in recipient ecosystems (Rabalais et al. 2002; Kemp et al. 2005). This elevated supply directly alters rates of N processing and cycling in terrestrial and aquatic ecosystems. Increased N can saturate biotic uptake causing ecosystems to retain a lower fraction of inputs (Aber et al. 1989; Bernot and Dodds 2005; Earl et al. 2006). The degree to which ecosystems respond with higher N transformation rates (e.g., denitrification) or storage (e.g., assimilatory uptake) will in part determine the extent of their alteration by excess N loading.

Streams and rivers play a central role in landscape-level N cycling because they can both transport N to other ecosystems and be hot spots in the landscape for N transformation, storage, and removal (McClain et al. 2003). Because only 10–25% of terrestrial N inputs reach the coastal ocean (Howarth et al. 1996; Schaefer and Alber 2007), even small changes in rates of N removal and storage as water makes it way through river networks may translate into large proportional changes in N flux to downstream ecosystems (Mulholland et al. 2008). Nitrate (NO_3^-) concentrations in surface waters vary over five orders of magnitude from <0.1 μg N L^{-1} in undisturbed catchments (Hedin et al. 1995) to $>10{,}000$ μg N L^{-1} in waters associated with substantial urban and agricultural land use (Royer et al. 2004). In N-polluted streams, NO_3^- is the dominant form of N export (Hedin et al. 1995; Royer et al. 2006) and excess NO_3^- can cause eutrophication or even be toxic in receiving streams and lakes (Dodds and Welch 2000). Assessing changes in NO_3^- removal from the water column, both as temporary assimilatory storage (i.e., in biomass) and permanent removal via denitrification is central to understanding how upstream processes may regulate delivery of bioreactive N to downstream ecosystems.

Nitrate uptake length, S_W, represents the average distance traveled by a NO_3^- ion prior to being removed from the water column and it is a primary metric for understanding NO_3^- removal from streams (Stream Solute Workshop 1990). The fate of this N varies; some N is denitrified (Mulholland et al. 2008), much is assimilated and quickly mineralized (Ashkenas et al. 2004), while another fraction is assimilated and retained in extended storage for >1 yr (Ashkenas et al. 2004). Despite 227 individual measurements of NO_3^- uptake length found in the literature (Tank et al. in press), we lack a general predictive model for the controls governing NO_3^- uptake length because most individual studies include only a few streams, and even fewer studies measure drivers that may control uptake length (e.g., carbon metabolism; Hall et al. 2003; Fellows et al. 2006).

Research to date shows several important controls on NO_3^- uptake length: (1) uptake length increases with stream size (measured as specific discharge, discharge/stream width [Q/w]), because faster, deeper streams carry nutrients farther downstream before removal by benthic processes (Peterson et al. 2001; Hall et al. 2002); (2) uptake lengths increase as greater dissolved inorganic N concentrations increasingly satiate biotic demand (Dodds et al. 2002; Earl et al. 2006; O'Brien et al. 2007); (3) biotic demand by algae and bacteria shorten NO_3^- uptake length (Hall and Tank 2003; Fellows et al. 2006; Newbold et al. 2006) and metabolic rates should in part be determined by N concentrations; and (4) land use will indirectly modify nutrient uptake, by altering metabolism (via effects on light and nutrients) or increasing inorganic N loading to the stream (Newbold et al. 2006).

As part of the Lotic Intersite Nitrogen eXperiment II (LINX II), we measured uptake lengths of $^{15}NO_3^-$ in 72 streams in eight regions to develop quantitative predictive models on controls of NO_3^- uptake length. We chose streams that spanned a range of extant land use and associated variation in NO_3^- concentration, geomorphology, and metabolism. The broad diversity of stream types and land uses fostered constructing quantitative relationships between predictor variables and NO_3^- uptake length. This paper expands on our findings that both denitrification and biological assimilation show a loss of efficiency of NO_3^- uptake with increasing NO_3^- concentration (Mulholland et al. 2008). Together with a companion study (Mulholland et al. 2009) that resolves rates and controls on denitrification in the same studied streams, our objective in this study was to estimate rates and controls of total NO_3^- removal by streams. We asked three questions: (1) How do NO_3^- uptake lengths and other uptake metrics vary across the 72 streams in United States and Puerto Rico? For this question, we used a comparative approach to evaluate how these rates compare with existing data (Tank et al. 2008). (2) How do specific discharge, NO_3^- concentration, and metabolism interact to control NO_3^- uptake lengths in streams and to what extent does land use interact with these factors to indirectly regulate NO_3^- uptake? We tested a model of controls on NO_3^- uptake length using structural equation modeling and previously identified control variables. In addition we expanded the model to include land use in order to examine indirect pathways by which land use alters NO_3^- uptake. Structural equation modeling allows testing a hypothesized pattern of causation with data. By comparing the actual covariance structure of the data with the covariance structure that would exist based on the hypothesized model, we can examine both whether the model is consistent with the data and also measure the coefficients of direct and indirect pathways. (3) To what degree do other measured biotic, chemical, and hydrological variables, beyond those in the structural equation models, improve predictions of NO_3^- uptake length? Because we did not have a priori causal and structural predictions for all of these variables, we constructed multiple regression models and evaluated them using Akaike's Information Criterion (AIC; Burnham and Anderson 2002).

Methods

Study sites—We selected 72 streams, encompassing nine streams in each of eight regional sites (Fig. 1). Within each region we categorized streams into each of three land-use types (native, agricultural, or suburban–urban-dominated catchments) based upon near-stream observations and catchment analysis of land use using a geographic information system. Streams draining native vegetation (hereafter

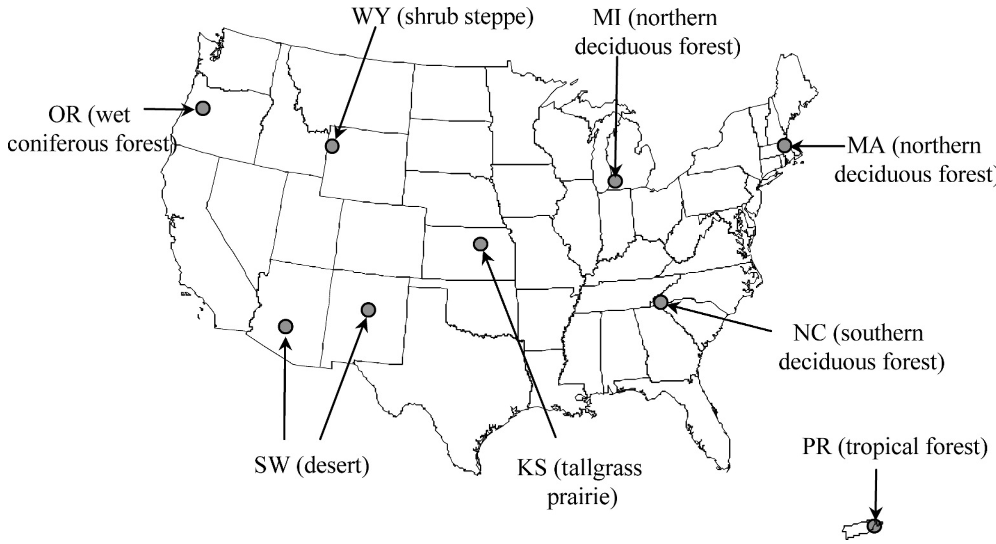

Fig. 1. The 72 study sites were located in eight regions across the United States and Puerto Rico representing six biomes. Abbreviations are Oregon (OR), Wyoming (WY), Michigan (MI), Massachusetts (MA), North Carolina (NC), Puerto Rico (PR), Kansas (KS), and Southwest (SW).

referred to as reference streams) varied according to biome and were dominated by local vegetation (e.g., forests, desert scrub, shrub-land, or grassland). Agricultural streams also varied regionally and included row-crop agriculture, pasture, and open range. Suburban–urban streams drained suburban housing, condominiums, dense urban areas, community parks and playfields, and golf courses. For each of the 72 streams, we quantified land use in each catchment using United States Geological Survey land-cover classifications (Mulholland et al. 2008). In this paper we use a single metric of land-use intensity, the fraction of catchment area in suburban–urban and agricultural land uses combined. Selected study streams were generally small but there was a broad range in both discharge (median discharge during the experimental addition was 18 L s^{-1}, and ranged from 0.2 L s^{-1} to 270 L s^{-1}) and NO_3^- concentration at the time of the experiment ranged 200,000-fold from 0.1 μg NO_3–N L^{-1} to 21,000 μg NO_3–N L^{-1}.

$^{15}NO_3$ injections, sampling, and analysis—We measured NO_3^- removal using 72 stable N isotope tracer additions; protocols are detailed in the online appendices to Mulholland et al. (2008) and briefly summarized here. We continuously injected $K^{15}NO_3$ and a conservative tracer (NaCl or NaBr) using a fluid-metering or peristaltic pump into each of the 72 streams for 24 h with injections beginning at 12:00–13:00 h local time. The target $\delta^{15}N$ value of the NO_3^- pool was +20,000‰, corresponding to a relatively modest 7.5% increase in the total NO_3^- concentration across all sites. We conducted these experiments during the time of year with high biological activity (i.e., spring and summer).

In each stream, we sampled $^{15}NO_3^-$ at six stations downstream from the addition point to measure the decline in ^{15}N tracer flux. We sampled immediately prior to the addition, and at 12 h and 23 h into each addition to compare ^{15}N–NO_3^- uptake diurnally. At each station we collected filtered water samples to measure NO_3^-, $\delta^{15}NO_3^-$, and conservative tracer concentration (Br^- or Cl^-).

We sampled ^{15}N–NO_3^- concentration by filtering 0.1–2 L water in the field. In the laboratory we added a known amount of unlabelled KNO_3 to each sample to dilute the estimated $\delta^{15}N$–NO_3^- from 20,000‰ to ~4000‰ for analytical purposes. For streams with low NO_3^- concentration, KNO_3 dilution had the added benefit of increasing N mass to the detectable range (~20 μg N) for mass spectrometry. We then added 3 g MgO and 5 g NaCl to each sample and reduced the volume to ~0.1 L by boiling following Sigman et al. (1997). After cooling we poured each sample into a 250-mL polyethylene bottle from which we suspended an acidified (0.063 mmol $KHSO_4$), 10-mm glass-fiber filter sandwiched between two 25-mm Teflon filters. We added 5 g Devarda's alloy to reduce NO_3^- to NH_3 and immediately sealed the bottle. Bottles were incubated for 1 week on a shaker table in order to diffuse NH_3 from the aqueous solution onto the acidified filter as NH_4^+ (Sigman et al. 1997). Following incubation we removed the acidified filters from their Teflon sandwiches, dried them in an acid desiccator and sealed them in tin capsules for mass spectrometer analysis. We analyzed samples for ^{15}N using either a PDZ Europa 20–20 instrument at the Marine Biological Laboratory in Woods Hole, Massachusetts , a PDZ Europa 20–20 instrument at University of California, Davis, or a ThermoFinnigan Delta Plus at Kansas State University.

Isotopic values are reported as $\delta^{15}N$ where $\delta^{15}N$ (‰) = $[(R_{samp}/R_{std}) - 1]1000$, R_{samp} is the $^{15}N/^{14}N$ of the sample and R_{std} is the $^{15}N/^{14}N$ of the standard, atmospheric N_2. We converted $\delta^{15}N$ to mole fraction (*MF*; $^{15}N/(^{14}N + ^{15}N)$). Mole fraction excess of NO_3^- was calculated by subtracting out ambient *MF* of NO_3^- (near 0.003663). We calculated excess concentration of ^{15}N excess of NO_3^- at each station downstream of the addition site by multiplying

MF excess by the measured NO_3^- concentration at that station. We then calculated the flux of $^{15}NO_3^-$ at each station by multiplying $^{15}NO_3^-$ concentration by discharge measured as dilution of the added conservative tracer (Br^- or Cl^-).

Associated field measurements—At each site we measured a suite of biotic and abiotic variables to statistically relate them to NO_3^- uptake including: temperature using data sondes; canopy cover estimated using a densiometer at 10 transects along each study reach; wetted stream width at 5–10-m intervals; velocity, estimated as the time to half-plateau concentration during conservative tracer additions; mean depth calculated as discharge/(width × velocity); and the size of transient storage zone estimated by fitting a one-dimensional advection, dispersion, and transient storage model to conservative tracer data (Runkel 1998). During metabolism measurement (described below) we continuously recorded photosynthetically active radiation at one point near the stream.

Chemical measurements included NO_3^- concentration, measured using ion chromatography or colorimetry; NH_4^+, measured using indophenol colorimetry or fluorometry; soluble reactive phosphorus (SRP) measured using molybdate-blue colorimetry. Each macronutrient was measured at every station along the reach, and for N species, during both day and night. We also measured dissolved organic carbon using high-temperature combustion on a Shimadzu TOC analyzer.

We measured both functional (metabolism) and structural (e.g., algal standing stocks) attributes of stream biota. Gross primary production (GPP) and ecosystem respiration (ER) were measured using open-channel diel oxygen budgets (Odum 1956; M. J. Bernot unpubl.). Oxygen exchange was measured using tracer gas injections (SF_6 or propane) following the 24-h stable isotope addition (Wanninkhof et al. 1990; Marzolf et al. 1994). In addition, we measured standing stocks of several benthic organic matter components (coarse and fine benthic organic matter, epilithon, bryophytes, filamentous algae, vascular plants) by quantitatively sampling them at 5–10 locations in each experimental stream reach. Samples were dried at 50°C and ashed at 500°C to convert to ash-free dry mass.

Data analysis—We calculated $^{15}NO_3^-$ uptake length (S_{Wtot}; i.e., the average distance traveled by a NO_3^- ion prior to removal from the water), using a first-order model (Newbold et al. 1981),

$$\ln {}^{15}NO^-_{3\ x} = \ln {}^{15}NO^-_{3\ 0} - k_{tot}x \quad (1)$$

where $^{15}NO^-_{3\ x}$ is $^{15}NO_3^-$ flux at meter x, $^{15}NO^-_{3\ 0}$ is flux at meter 0 (i.e., the tracer addition point), k_{tot} is the uptake rate (m^{-1}) and x is distance downstream (m). S_{Wtot} (m) is calculated as $1/k_{tot}$.

Uptake length is, in part, driven by depth and velocity because fast, deep streams will transport NO_3^- farther before uptake. We calculated uptake velocity (v_f, m min^{-1}) to compare uptake among streams with varying depths and velocities (Davis and Minshall 1999; Hall et al. 2002). Uptake velocity can be considered the demand for a nutrient relative to its concentration and is calculated as

$$v_f = Q \times k_{tot}/w \quad (2)$$

where Q is stream discharge (m^3 min^{-1}), and w is stream wetted width (m). Note that Q/w = velocity × depth. We used specific discharge as a metric of stream size because given a constant nutrient demand (i.e., constant v_f) uptake length S_{Wtot} should scale linearly with Q/w. The uptake velocity can be used to calculate the areal uptake flux U (mg N m^{-2} min^{-1}) which is the mass of N removed from water per area per time as

$$U = v_f \times \left[NO_3^-\right] \quad (3)$$

where $[NO_3^-]$ is the average ambient concentration of NO_3^- in stream water (mg N m^{-3}). We report U, but we focus on S_{Wtot} because it is calculated independently from two important predictor variables, Q/w and $[NO_3^-]$.

We $\log_{10}$-transformed non-fractional data prior to analysis because data were non-normally distributed with variance increasing with the mean. Land-use fractions were arcsine-square-root–transformed. To examine variation among regions and land-use categories we used two-way ANOVA with fixed effects. Diel differences in NO_3^- cycling metrics were examined using paired *t*-test. Bivariate regressions were estimated using ordinary least squares. All statistics were calculated using the statistical package R (R Development Core Team 2006).

We used two complementary multivariate statistical approaches. The first was structural equation modeling (SEM) using observed variables (Shipley 2000; Grace 2006), which is similar to path analysis. We used this approach because we had a priori hypotheses relating primary controls directly to S_{Wtot} (Fig. 2A; *see* Introduction). To this simple model we added human land use measured as fraction of area with agriculture + suburban–urban cover within each catchment (Fig. 2B). We modeled land use as an indirect effect (i.e., land use can only modify proximate variables such as riparian vegetation, stream morphology, or nutrient concentrations and not directly affect nutrient dynamics). Based on the resulting correlation tables, we found two correlations in exogenous variables for which we had no a priori hypotheses; therefore, we modeled these as unspecified covariances (*see* Results). Structural equation modeling tests this hypothesized causal model of controls on nutrient uptake and estimates coefficients for each path (Shipley 2000). Using the package *sem* in R, we fit the expected covariance matrix based on the path model to the covariance matrix derived from the data by iteratively solving for a maximum likelihood solution (Fox 2006; R Development Core Team 2006). We used a chi-square–based goodness-of-fit test where $p > 0.05$ showed that the model structure was consistent with the data. We report unstandardized coefficients, rather than standardized coefficients, which allows measuring the direct effect of a predictor (e.g., NO_3^- concentration) on a response variable (Grace 2006). To estimate the fraction of variation explained by the models, we calculated error variance for S_{Wtot} in a model with standardized coefficients.

We also evaluated a set of multiple linear regression (MLR) models to complement the SEM analysis. We addressed two specific questions to address with the MLR analysis. What other variables besides those identified a priori and included in the SEM analysis may serve as useful predictors of NO_3^- uptake? How does the predictive capability of correlative MLR models compare with structured causal-based models of NO_3^- uptake from SEM analysis?

We selected the set of MLR models using AIC, which balances model predictive ability and parsimony (Burnham and Anderson 2002). Relative differences between AIC values provide empirical support for individual MLR models in a candidate set (Burnham and Anderson 2002), and we applied a small sample size correction to AIC values (AIC_c) because of small sample size ($n = 59$; excluding missing values in explanatory terms; Burnham and Anderson 2002). The relatively small sample size implied that we would introduce substantial bias into the analysis if uncorrected AIC values were used. We used a stepwise procedure to select a set of MLR models that predicted S_{Wtot} with differences in AIC_c values (Δ_i) < 2.0. There were 19 variables describing hydrological, physical, chemical, and biological characteristics of study streams available for model selection. Additionally, we computed model likelihood [$L(g_i|x)$], relative model likelihood (w_i), and adjusted R^2 for each MLR model in the candidate set (Burnham and Anderson 2002).

Results

Bivariate relationships—For three of our study streams, we found no statistically significant decline in $^{15}NO_3^-$ flux downstream; therefore, they were excluded from further analysis. Among the 69 streams having significant downstream decline in $^{15}N–NO_3^-$ flux, uptake length, S_{Wtot}, varied considerably (median for 69 streams = 777 m, range = 20–18,000 m; Fig. 3). Uptake velocity (v_f) median for all streams was 0.42 mm min^{-1} and individual streams ranged from 0.024 mm min^{-1} to 17.9 mm min^{-1}. Uptake velocity varied among regions, but showed no relationship with the three land-use categories (2-way ANOVA, region $p <$ 0.001, land use $p = 0.34$, interaction, $p = 0.16$). Streams in Wyoming generally had the highest v_f, while those in Massachusetts were lowest (Fig. 3). Areal rates of NO_3^- uptake, quantified as U, varied both among sites and among the three land-use categories (2-way ANOVA, region $p = 0.006$, land use $p = 0.0009$), with the influence of land use being robust across regions (region by land use interaction, $p = 0.97$). Reference streams had lower U values than agricultural and suburban–urban streams. Mean areal NO_3^- uptake was highest in Michigan and Kansas and lowest in Oregon and Southwest streams; these patterns were driven primarily by differences in background NO_3^- concentration rather than differences in v_f (Fig. 3).

Uptake velocities of NO_3^-, although variable, fell within the range of 227 other previously published studies (Tank et al. 2008). Uptake velocity (v_f) declined as NO_3^- concentrations in our 69 streams increased (solid points in Fig. 4A; Mulholland et al. 2008). However, when solely considering the 227 previous NO_3^- uptake measurements (open points; Fig. 4A) no relationship existed between NO_3^- concentration and v_f (Fig. 4A). Uptake flux increased as NO_3^- concentrations increased, but a shallower slope than would be predicted based on the computation (Fig. 4B) showing fractional loss of uptake flux. The slope of the relationship between log v_f and log NO_3^- did not vary among the eight regions because there was no interaction between log NO_3^- and region (analysis of covariance [ANCOVA], log NO_3^- $p < 0.0001$, site $p = 0.006$, interaction $p = 0.48$), but the magnitude of v_f varied strongly among regions (Fig. 3). Similarly, the slope of log v_f vs. log NO_3^- did not vary among the three land-use categories (ANCOVA, log NO_3^- $p < 0.0001$, land use $p = 0.05$, interaction $p = 0.78$).

Past research has shown that diurnal and nocturnal values for v_f can differ because of the contribution of photoautotrophic assimilatory demand for NO_3^- (Mulholland et al. 2006). Daytime values of log v_f (m min^{-1}) averaged 0.07 higher than night (paired t-test, $p = 0.038$) which indicates that v_f averaged about 20% higher during the day than at night. However, there was considerable variability in the diel relationship in v_f with 16 of 53 paired measurements lower during day than during night. Moreover, the amount of fractional change in v_f from day to night did not significantly correlate with GPP or NO_3^-.

Using simple linear regression analysis, land use expressed continuously as the fraction of catchment area in agriculture + urban land use explained only 5% of the variation in v_f. (Fig. 5). Land use more strongly predicted areal uptake rate (U), with U increasing as human land use increased (Fig. 5), a pattern likely driven by higher stream NO_3^- concentrations in catchments with greater human-influenced land cover (Fig. 6). Streams with high fractions of human land use tended to also have higher GPP (Fig. 6).

Multivariate controls of $S_{w\text{-}tot}$—Structural equation modeling identified some significant causal relationships between predictor variables and S_{Wtot}. Our hypothesized causal model of the controls on NO_3^- uptake was consistent with the data (χ^2 test $p = 0.72$, df = 3; Fig. 7A) and this SEM model explained 79% of the variance in log S_{Wtot}. Significant paths to S_{Wtot} included those from Q/w, NO_3^-, NH_4^+, and GPP. Ammonium and NO_3^- concentrations did not affect metabolic rates and the path from ER to S_{Wtot} was not significant demonstrating that metabolic control of S_{Wtot} was solely via GPP.

Path parameters can provide information on the functional relationships between controls and S_{Wtot}. Those in the simple model (Fig. 7A) are based on log-transformed data; hence, the coefficients are exponential in scaling relationships between predictor variables, with a slope of 1 indicating linear increase and slope between 0 and 1 indicating an increasing, but attenuating, relationship. For example, the path parameter between NO_3^- and S_{Wtot} was 0.36, showing that S_{Wtot} lengthens as NO_3^- concentrations increase, indicating a loss in overall uptake efficiency (O'Brien et al. 2007; Mulholland et al. 2008). The path parameter for the effect of Q/w on S_{Wtot} was 0.61 indicating that uptake lengths increased less rapidly relative to increasing Q/w. Expected value for the path parameter was 1 because S_{Wtot} should increase linearly with Q/w. We

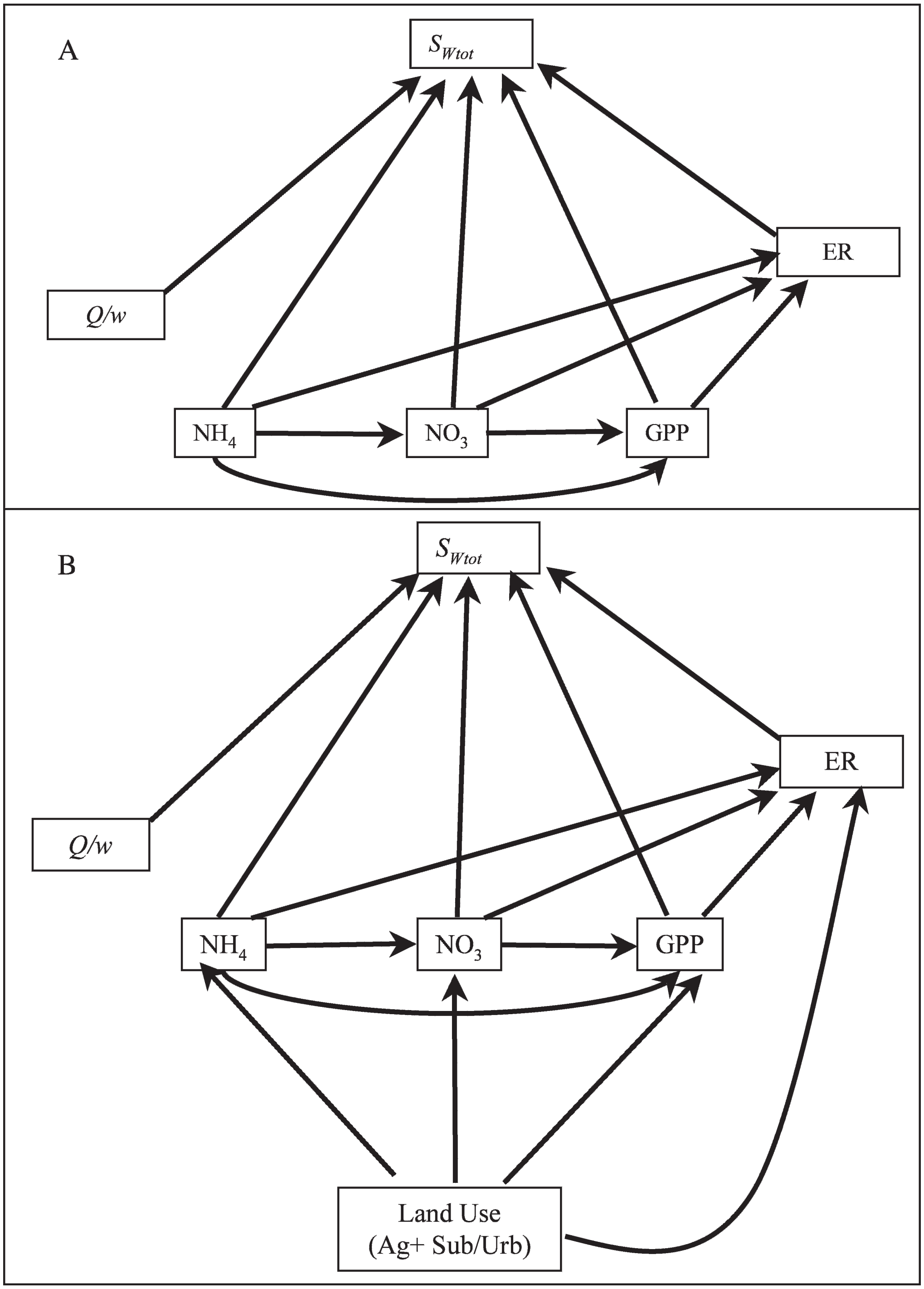

Fig. 2. Hypothesized causal models describing controls of NO_3^- uptake length (S_{Wtot}). Boxes are variables in the models. Arrows are hypothesized causal relationships. Panel A is the simple model. Panel B describes a more complex model where changes in land use affect controls on nitrogen cycling. GPP = gross primary productivity, ER = ecosystem respiration, NO_3 = nitrate concentration, NH_4 = ammonium concentration, Q/w =specific discharge, and land use = the fraction of catchment area in agricultural + suburban–urban land cover. For specifics on hypothesis generation, *see* Introduction.

tested the model fit by fixing the parameter from Q/w to S_{Wtot} to 1; model fit was poor (χ^2 test $p < 0.001$), showing that monotonic increase in S_{Wtot} with Q/w did not match the data well.

Including human land use (i.e., the fraction of land area under agricultural and suburban–urban land uses) in the SEM model also produced a model consistent with the data (χ^2 test $p = 0.45$, df $= 4$; Fig. 7B). Human land-use intensity increased rates of GPP. Additionally, streams with greater fractions of human land use had higher NO_3^- and NH_4^+ concentrations. Parameter estimates for paths from GPP and NO_3^- to S_{Wtot} were of equal magnitude, but of

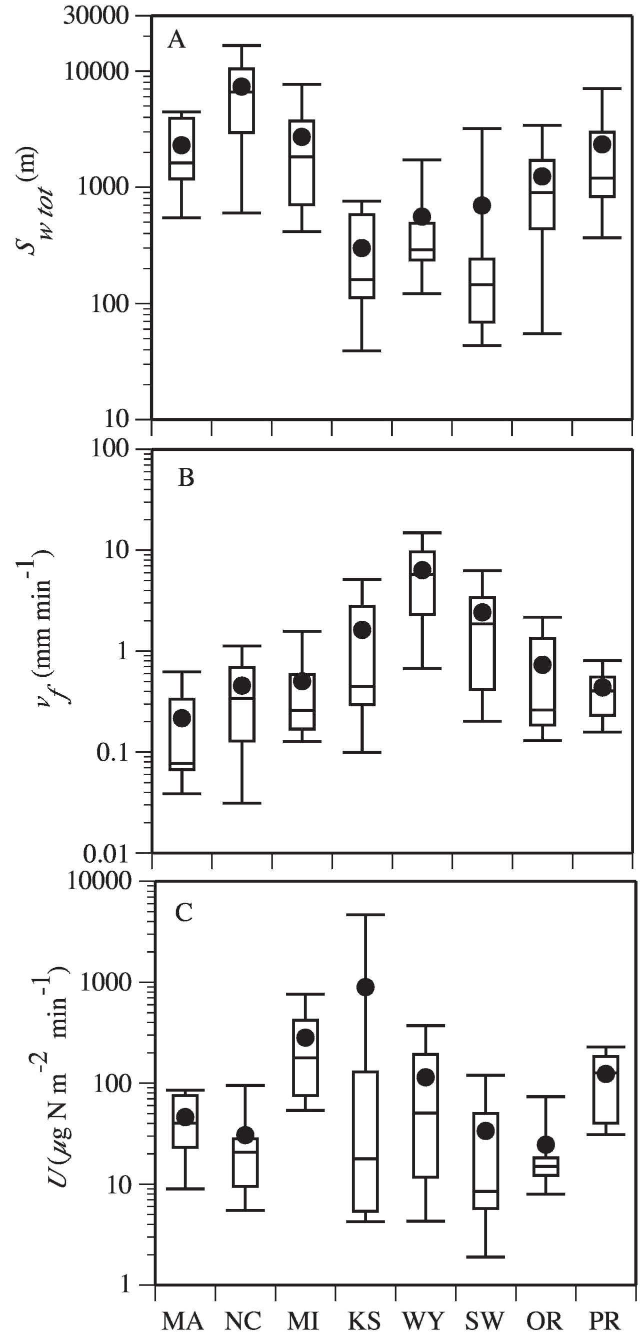

Fig. 3. (A) Nitrate uptake length (S_{Wtot}), (B) uptake velocity (v_f), and (C) uptake flux (U) varied greatly among the sites. Box-and-whisker plots indicate mean (dot), 50th percentile (line in box), 25th and 75th percentiles (boxes), and 10th and 90th percentiles (whiskers). Abbreviations for sites are the same as on Fig. 1.

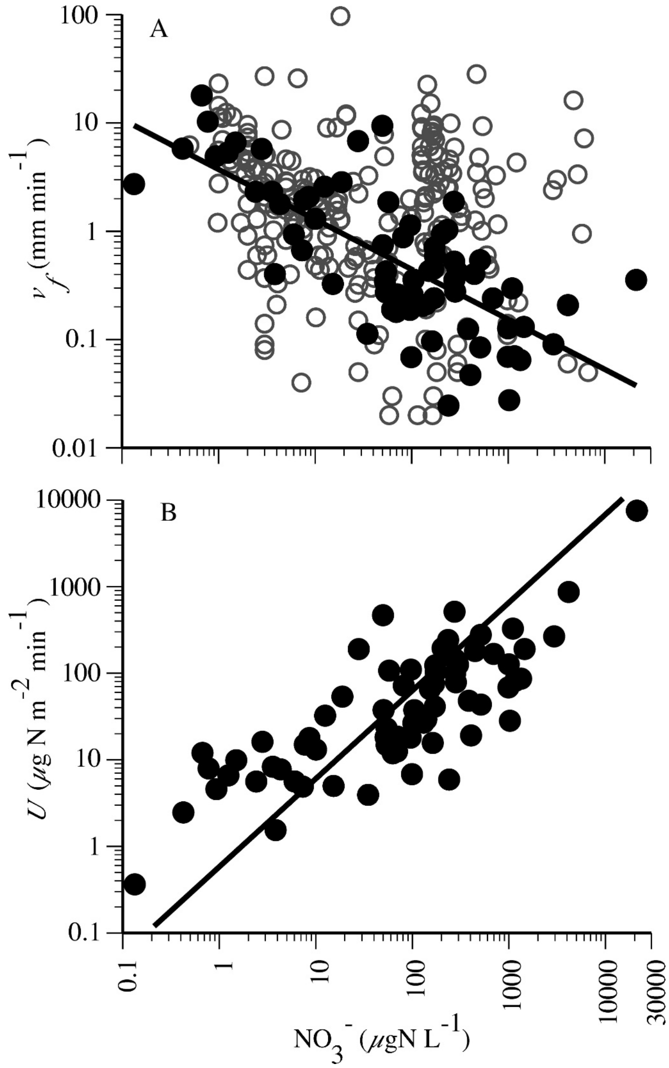

Fig. 4. (A) Nitrate uptake velocity (v_f, mm min^{-1}) declined with increasing NO_3^- concentration in the 69 streams in this study where NO_3^- removal was measurable (solid points). Line is least-squares linear regression fit only to the 69 streams in this study. Equation is log v_f =log[NO_3^-] $\times$ $-0.462 + 0.574$. Grey points are 227 other studies summarized from Tank et al. (2008). (B) Nitrate uptake flux (U; μg N m^{-2} min^{-1}) increased with NO_3^- concentration as expected because U = [NO_3^-] $\times$ v_f. The plotted 1 : 1 line shows expected relationship based on computation alone.

opposite sign, meaning that the overall effect of land use was to effectively cancel out its indirect influence on S_{Wtot}.

Multiple linear regression models selected according to AIC$_c$ criteria contained similar variables as the SEM model for S_{Wtot} (Table 1). All five selected models ($\Delta_i < 4.0$ of top model) included stream slope, discharge, stream width, NO_3^- concentration, NH_4^+ concentration, and GPP. Additionally, ER and F_{med}^{200}, a metric of transient water storage (Runkel 2002), were present in four of the five most consistent models. Riparian shade and SRP concentration occurred in one model each. However, likelihoods and weights (Table 1) for these two models were nearly identical to the model with the least number of explanatory variables, suggesting that including these two variables was a statistical artifact. In all models, multiple R^2 was ~0.83, which was only 0.04 units higher than the SEM model. Adjusted R^2 values for these models were 0.79–0.80 (Table 1).

Discussion

Uptake length of NO_3^- was strongly regulated by the combination of physical (specific discharge, Q/w), chemical

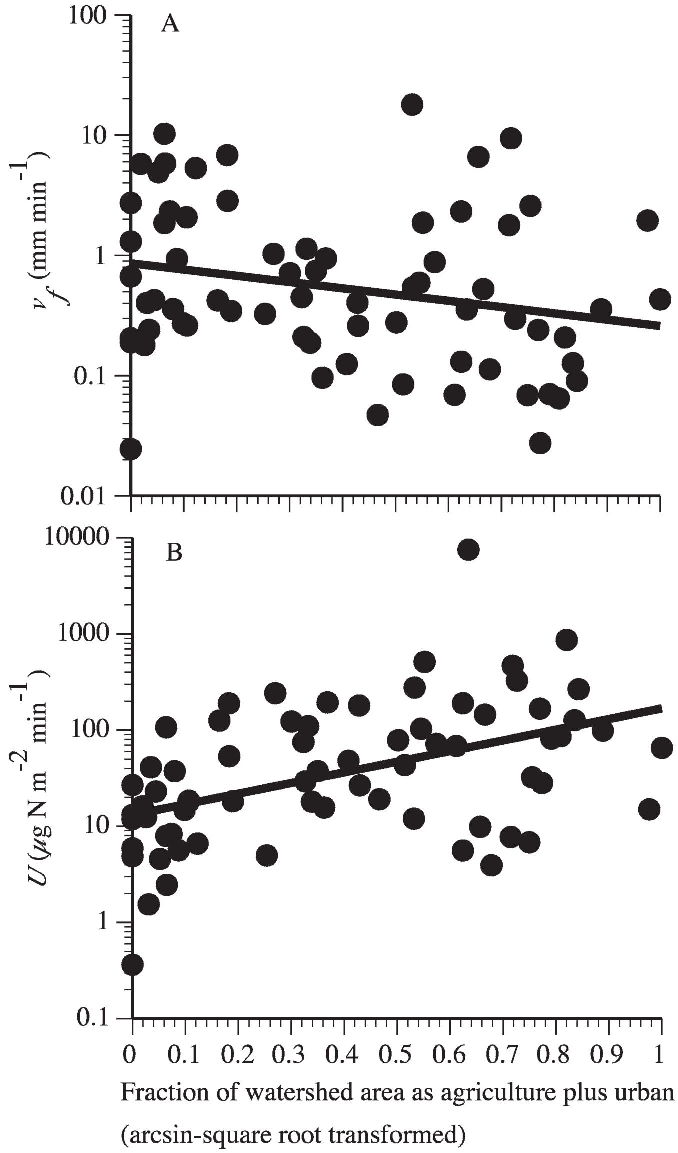

Fig. 5. (A) log nitrate (NO_3^-) uptake velocity (v_f) declined slightly and (B) NO_3^- uptake flux (U) increased as a function of land use, measured as the arcsine-square-root–transformed fraction of watershed area in both suburban and urban and agricultural human land use (lu). Lines are least-squares linear regressions with the equations log $v_f = -0.52 \times lu - 0.65$, $p = 0.04$, $r^2 = 0.05$ and log $U = 1.11 \times lu + 1.12$, $p < 0.0001$, $r^2 = 0.19$.

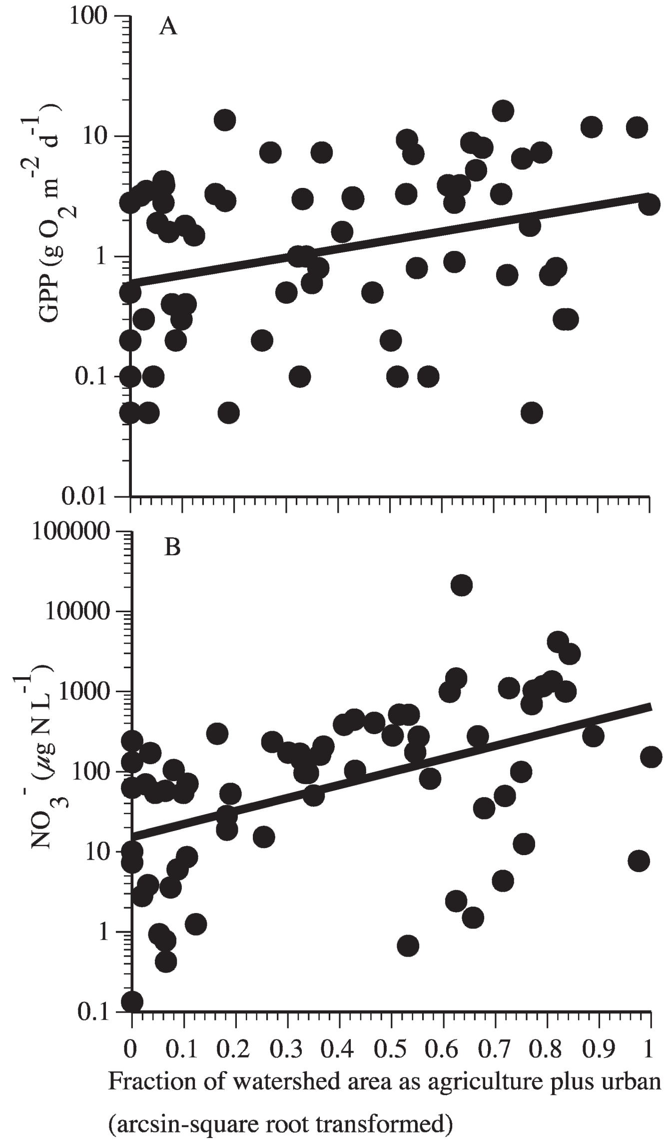

Fig. 6. (A) Gross primary production (GPP) and (B) NO_3^- concentration were positively related to proportions of suburban and urban and agricultural land use, measured as arcsine-square-root–transformed fraction of watershed area in both suburban and urban and agricultural human land use (lu). Lines are least-squares linear regressions with the equations log GPP $= lu \times 0.72 - 0.22$, $p = 0.012$, $r^2 = 0.09$, and log[NO_3^-] $= lu \times 1.62 + 1.18$, $p < 0.0001$, $r^2 = 0.21$.

(stream water NO_3^- concentration), and biological (GPP) factors. Together, these three factors explained nearly 80% of the variation in log S_{Wtot} based on measurements made in 69 streams spanning a wide range of physical and chemical properties. Having such a large number of streams where ^{15}N–NO_3^- tracer experiments were all conducted with the same methods allowed for increased statistical power in the face of the high background variability inherent in studies of nutrient cycling in streams (Simon et al. 2005).

Multiple regressions with AIC model selection included the same variables we chose a priori for the causal-based SEM approach. The MLR analysis suggested that other variables related to channel hydraulics (i.e., F_{med}^{200}, slope) could explain some additional variation in log S_{Wtot}. However, these more complex models explained only 4% more variation than the SEM; thus, their additional complexity provided only a small increase in predictive capability.

Direct controls on NO_3^- removal—As expected, S_{Wtot} lengthened as stream size increased, as previously noted in other studies examining the relationship of S_{Wtot} with Q/w (Wollheim et al. 2001; Hall et al. 2002) and Q (Peterson et

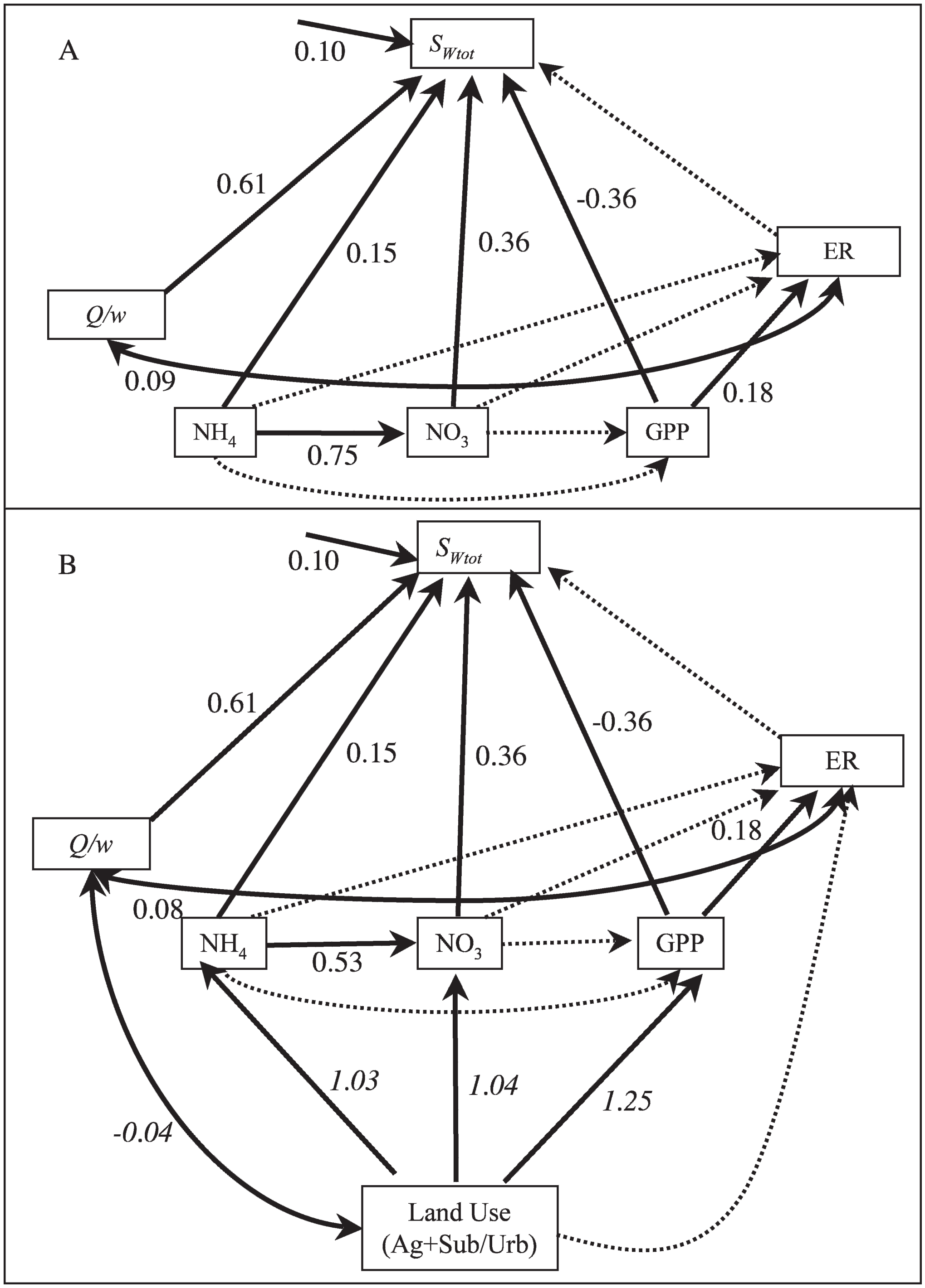

Fig. 7. Structural equation models describing controls of NO_3^- uptake length (S_{Wtot}). Panel A is the simple model. Panel B describes a more complex model where changes in land use affect controls on nitrogen cycling. Boxes are variables in the models. Single-headed, solid arrows are paths that are signficantly different than 0, $p < 0.05$, and dotted arrows are hypothesized paths that were not significant. Double-headed arrows are unhypothesized covariances. Numbers are unstandardized path coefficients. Error variance was calculated for all variables, and is shown for S_{Wtot}. Italicized path coefficients leading from land use are not to be interpreted as power–law coefficients because land use was arcsine-square-root–transformed. Abbreviations follow those in Fig. 2.

al. 2001; Tank et al. 2008). Although our streams were not large (max. Q was 270 L s^{-1}), discharge ranged 300-fold across the 72 streams. A surprising finding is that the parameter estimate between Q/w and S_{Wtot} was 0.61, significantly lower than 1 (Fig. 7A). We expected that S_{Wtot} would increase linearly with Q/w, yielding a parameter estimate of 1 with log–log data. Instead the parameter was <1 showing that S_{Wtot} increased more slowly than stream size. Model fit with the parameter fixed to 1 was poor. This finding implies that larger streams have

Table 1. Multiple linear regression models chosen with Akaike's Information Criterion adjusted for small samples size (AIC_c) predicting log_{10}-transformed NO_3–N uptake length (S_w). Shown are the five best models where Δ_i $AIC_c < 2.0$. The term $L(g_i|x)$ is the probability that a particular model is the best given available data; w_i is the evidence that an individual model is the best among the competing models (all w_i terms sum to 1) assuming that the best model occurs in the candidate set (Burnham and Anderson 2002).

Rank	Model covariates*	AIC_c	Δ_i AIC_c	Likelihood $L(g_i|x)$	w_i	Adj. R^2
1	GRAD, Q, w, FM200, NO_3^-, NH_4^+, GPP, ER	−130.17	0.00	1.00	0.33	0.80
2	GRAD, Q, w, FM200, NO_3, NH_4^+, GPP	−129.69	0.48	0.79	0.26	0.80
3	GRAD, Q, w, FM200, NO_3^-, NH_4^+, GPP, ER, shade	−128.50	1.66	0.44	0.14	0.80
4	GRAD, Q, w, NO_3^-, NH_4^+, GPP, ER	−128.47	1.70	0.43	0.14	0.79
5	GRAD, Q, w, FM200, NO_3^-, NH_4^+, GPP, ER, SRP	−128.24	1.93	0.38	0.13	0.80

* GRAD = stream gradient; Q = discharge; w = stream width; FM200 = $F_{med}{}^{200}$; NO_3^- = NO_3–N concentration; NH_4^+ = NH_4–N concentration; GPP = reach-scale gross primary production; ER = ecosystem respiration; shade = riparian canopy cover; SRP = soluble reactive phosphorus. All covariates were log_{10}-transformed prior to analysis. Not listed are alternative models with a Δ_i $AIC_c > 2.0$; Δ_i $AIC_c = AIC_{c,i} - AIC_{c,1}$ where i is model rank.

relatively higher v_f for NO_3^- than smaller ones, and that this effect of stream size is independent of GPP and NO_3^-. We might expect greater rates of GPP in larger streams due to decreased channel shading (Vannote et al. 1980), but this effect is addressed independently by the multivariate SEM. Additionally Q/w and GPP were uncorrelated, so it is a mystery as to why, in our sample of 69 small streams, S_{Wtot} increased nonlinearly with increasing Q/w. It is possible that larger streams have geomorphic characters that could confer higher uptake rates. This possibility merits further study as well as other potential mechanisms controlling S_{Wtot} across a range of stream sizes.

The efficiency of NO_3^- removal declined as stream water NO_3^- concentrations increased (Figs. 4, 7). If the parameter value from the SEM analysis between NO_3^- and S_{Wtot} were 0 then streams would have infinite capacity to take up excess NO_3^- and, therefore, uptake (U) would have increased monotonically as NO_3^- concentrations increased. If the SEM parameter were 1, streams would have no excess biological processing capacity for NO_3^- and U would be constant across a range of NO_3^- concentration. Instead, the parameter value for NO_3^- concentration and S_{Wtot} was between these two extremes at 0.36 (Fig. 7), indicating a loss in efficiency for NO_3^- removal even while more NO_3^- is being removed. This loss in efficiency causes increased uptake length; for each 10-fold increase in NO_3^- concentration, uptake length increases 2.3-fold (i.e., $10^{0.36}$). As an example, if a 1-km reach had an uptake length for NO_3^- of 5 km, then 18% of the NO_3^- load would be removed; but a 10-fold increase in NO_3^- concentration would reduce NO_3^- removal to only 8%, representing about a 2-fold decline in removal efficiency.

The effect of declining nutrient uptake efficiency (as v_f) with increasing NO_3^- concentration (Fig. 4) has been observed in other studies using approaches that examine variation in ambient streamwater nutrient concentration (Dodds et al. 2002) as well as through short-term enrichment experiments, a method that can saturate uptake (Earl et al. 2006). However, the pattern we observed of declining v_f with increasing NO_3^- concentration was not evident in the review of 227 previously published studies (Tank et al. 2008) even though the range of NO_3^- concentrations overlapped (Fig. 4). This finding suggests that meta-analyses of existing studies of NO_3^- uptake, most of which use the nutrient enrichment approach, may be less powerful in elucidating mechanisms controlling NO_3^- uptake. It is well-documented that solute releases involving experimental manipulations of nutrients alter absolute (U) and relative (v_f) rates of uptake (Mulholland et al. 2002; Earl et al. 2006). In the first LINX project addressing N dynamics in 11 streams (Peterson et al. 2001), comparison of S_W for NH_4^+ derived first by enrichment and later via ^{15}N release showed that enrichment reduced v_f 2–20-fold for a given stream (Mulholland et al. 2002). In our study of 69 streams, v_f for NO_3^- was less variable than those quantified by increasing NO_3^- concentration. Thus, assessment of uptake metrics derived from enrichment approaches may fit poorly with ambient measures of N availability as indicated by our larger assessment of previous studies. At least as important, however, is the fact that isotopic-tracer methods allows us to detect much smaller relative declines in flux and accurately represent N processing in streams with little N capital. Lastly, we used standardized techniques across all 69 studied streams, which is not the case for previously published values.

Even though NO_3^- uptake efficiency (as v_f) declined as NO_3^- concentration increased, the slope of log v_f vs. log NO_3^- concentration never declined to −1 meaning that there was no point at which high NO_3^- concentrations completely saturated uptake (O'Brien et al. 2007). If uptake flux (U) were saturated, then, v_f would decline monotonically with increasing NO_3^- concentration. Despite the strong loss in efficiency of removal as NO_3^- concentration increased, even streams with the highest concentrations removed NO_3^- at higher total rates than streams with lower concentrations, albeit at a lower fractional removal rate. The three streams for which we could not measure uptake had concentrations of 4, 112, and 154 µg NO_3–N L^{-1}, which were below or near the median NO_3^- concentration of 115 μg NO_3–N L^{-1}.

Gross primary production strongly regulated S_{Wtot} with high rates of GPP shortening S_{Wtot}. The parameter estimate from the SEM analysis was −0.36 (Fig. 7) showing a negative attenuating relationship between GPP and NO_3^- uptake. For a 10-fold increase in GPP, uptake length will decline by 2.3-fold. The effect of ER on S_{Wtot} was not significant, demonstrating that autotrophic processes played a stronger role in NO_3^- uptake, mostly as assimilatory demand (Mulholland et al. 2008). This relationship is consistent with stoichiometric expectations, because higher rates of C fixation drive higher assimilatory demand for N (Hall and Tank 2003; Mulholland et al. 2006). Interestingly, when the denitrified fraction of NO_3^- uptake was considered separately, ER was significantly related to dentrification in the same streams (Mulholland et al. 2009), demonstrating that heterotrophic activity more strongly regulates the dissimilatory component of NO_3^- removal. The positive effect of GPP on NO_3^- uptake has been noted in other studies; GPP was positively related to NO_3^- v_f in streams in Grand Teton National Park (Wyoming) while ER was not (Hall and Tank 2003). Also using the ^{15}N tracer approach, Mulholland et al. (2006) showed that NO_3^- uptake was related to seasonal and day-to-day variations in GPP produced by differences in light availability in a small, forested stream. Nitrate v_f was positively related to both GPP and ER in four streams spanning a gradient in light availability, although the relationship with ER was much weaker (Fellows et al. 2006). Ammonium v_f in New York streams was positively related with both GPP and ER (Newbold et al. 2006). However, not all studies have found a positive relationship between GPP and nitrogen uptake. Nitrate v_f was positively related to ER, but not to GPP in three forested streams in the Upper Peninsula of Michigan (Hollein et al. 2007). A multisite $^{15}NH_4^+$ tracer study among 10 streams found no relationship between ecosystem metabolism and NH_4^+ v_f (Webster et al. 2003). Given these variable results, it is possible that in some studies there are not enough replicates to provide suitable statistical power to detect relationships between uptake and GPP (Webster et al. 2003). With the 69 streams included in this study, multivariate methods were able to isolate the controlling role of GPP, along with stream size and NO_3^- concentration on S_{Wtot}.

Given the strong effect of GPP on S_{Wtot}, daily variation in light should drive diel variation in S_{Wtot}, with shorter uptake lengths during the daylight reflecting C fixation and assimilatory reduction of NO_3^- (Mulholland et al. 2006). Surprisingly, despite a trend toward higher v_f (i.e., shorter S_{Wtot}) during the day, the pattern was not ubiquitous; about one-third of the streams had lower v_f during the day. Additionally, the change in v_f between night and day was not related to the magnitude of GPP, which contradicted our expectation that streams with higher GPP should also have greater diel variation in NO_3^- demand. Few published comparisons of NO_3^- uptake during day vs. night are available. Using elevated NO_3^- additions, Fellows et al. (2006) found that uptake was higher during the day in four streams, but the difference was not statistically significant for any one stream, which is consistent with our findings. In contrast, Mulholland et al. (2006), using $^{15}NO_3^-$ tracer addition approach, found that peak daytime uptake was at least twice night uptake in early spring when light levels were high, but there was little diel difference during summer when light levels were low in this closed-canopy forested stream. It is possible that increased demand for NO_3^- as an electron acceptor (e.g., via denitrification) at night when oxygen is lower might reduce the difference in demand between day vs. night; but, we observed little diel variation in denitrification rates across our 69 streams (Mulholland et al. 2009). In addition, with denitrification averaging 16% of total uptake (Mulholland et al. 2008), variation in assimilatory demand should drive variation in total NO_3^- removal rather than variation in denitrification. Alternatively, NO_3^- uptake rates may decline slowly at night as recently fixed photosynthate is gradually depleted, and our midnight measurements of uptake may not reflect peak differences between day and night uptake (Mulholland et al. 2006).

Indirect effect of land use—Land-use categorization was not immediately apparent as an attribute controlling NO_3^- uptake. Uptake velocity varied little among our three assigned land-use categories and human land cover only weakly predicted v_f in a linear regression (Fig. 5). Further, land use did not appear as a significant predictor in multiple regression models. Based on these findings, it is tempting to conclude that land use had only a small effect on rates of NO_3^- uptake in streams. However, SEM demonstrated that land use in fact had strong, but largely indirect effects on N dynamics. Streams in areas of high suburban–urban or agricultural land cover had higher NO_3^- concentrations presumably as a result of anthropogenic loading via fertilizer application. These same streams also had higher GPP likely because of decreased shading due to a lack of riparian vegetation along agricultural streams (M. J. Bernot unpubl.). Increased GPP shortened S_{Wtot}, whereas increased NO_3^- concentrations lengthened S_{Wtot}, thus canceling out the overall effect of land use on S_{Wtot}. The effect of land use was strong, but ultimately had no net effect on S_{Wtot}. These results demonstrate the strength of the SEM approach for increasing understanding of causal relationships in stream nutrient cycling; this technique revealed indirect causes of land use on NO_3^- uptake, even if the net effect was small. These findings consider the entire sample of 69 streams. In particular regions or streams the counteracting effects of land use might not be so balanced, and land use could then strongly influence N biogeochemistry; for example, percentage forest cover was positively related with NH_4^+ v_f in 10 catchments in New York (Newbold et al. 2006).

A caveat of this research is that it represents a snapshot of N cycling conducted at baseflow during the biologically active season. By necessity, in order to compare among 72 streams we imposed this restriction. However, hydrologic variability certainly will drive variation in N cycling among streams. For example, urban streams tend to be much flashier hydrologically (Paul and Meyer 2001); thus, they may be expected to be much less retentive of N over longer time scales. Future research should incorporate hydrologic variability, preferably in studies using isotope tracers that assess longer term fate of tracers (Ashkenas et al. 2004).

This study clearly demonstrates that streams, even those altered by humans, can remove NO_3^- from transport. However these streams removed a smaller fraction of their NO_3^- load as NO_3^- concentrations increased. Streams became less efficient at NO_3^- removal (O'Brien et al. 2007; Mulholland et al. 2008) causing uptake lengths to increase 2.3 times with each 10-fold increase in NO_3^-. By having many replicates and identical methods, closely coordinated studies such as ours can elucidate relationships that may not be apparent in meta-analyses. Models that consider NO_3^- loss from streams in an effort to predict export to downstream ecosystems should consider the role of NO_3^- concentration in regulating this removal rate (Mulholland et al. 2008). Variability of v_f was high and far exceeded the range of simulated v_f used in other modeling efforts such as Wollheim et al. (2006). Our results provide a means to link physical and biological mechanisms of N cycling to observed patterns in net NO_3^- removal in river networks (Alexander et al. 2000; Bernhardt et al. 2005; Gruber and Galloway 2008). Using the empirical models we have developed can reduce uncertainty in predictions from watershed export models.

An important finding is that most NO_3^- removal in streams is not a result of denitrification, but rather due to uptake via assimilatory processes (Mulholland et al. 2009). Although denitrified N is permanently lost from the stream, it averages only 16% of total NO_3^- uptake (Mulholland et al. 2008). The ultimate fate of the remaining assimilated NO_3^-–N is unknown, but includes mineralization within a few weeks (Ashkenas et al. 2004), or exported as dissolved organic nitrogen (DON) (L. T. Johnson unpubl.) or particulate matter. Some NO_3^- may enter hyporheic zones (Triska et al. 1989) and depositional areas (Bernot and Dodds 2005) where some of the N may be stored for >1 yr (Ashkenas et al. 2004). Unlike denitrification this N is not permanently removed from the stream, but rather stored for variable periods. Nonetheless this assimilatory uptake and storage should contribute to downstream water quality because much of assimilated N is not moving downstream. The degree to which this assimilated N will contribute to downstream flux of N will depend on DON production and benthic seston suspension and transport (Newbold et al. 2005). Although assimilated N is not permanently lost from the stream, assimilation will retard downstream transport of NO_3^- from streams before it can be denitrified. Given that 16% of removed NO_3^- is denitrified, in just six spirals, denitrification will permanently remove NO_3^-. In addition, some fraction of assimilated NO_3^- may be both mineralized and quickly denitrified entirely within stream sediments, via coupled nitrification–denitrification (Seitzinger et al. 2002). Finally, assimilated N also could be transported to reservoirs during floods, where it may be ultimately buried or denitrified (Alexander et al. 2002; Seitzinger et al. 2002). Assimilation of NO_3^- by stream biota can increase the degree to which streams function as sinks for N in the landscape both by slowing down NO_3^- transport prior to denitrification and by the potential for long-term storage.

Acknowledgments

This work was supported by U.S. National Science Foundation (NSF) grant DEB-0111410 to the University of Tennessee, Knoxville, several NSF Long Term Ecological Research (LTER) grants to some of the individual sites, and numerous smaller grants and fellowships to a number of participating institutions. We thank more than 100 students and scientists who gathered data that contributed to this synthesis. We also thank the NSF LTER network, U.S. Forest Service, National Park Service, local municipalities, and many private landowners for permission to conduct experiments on lands they control. Dolly Gudder and two anonymous reviewers provided constructive comments that improved earlier versions of this manuscript.

References

Aber, J. D., K. J. Nadelhoffer, P. Steudler, and J. M. Melillo. 1989. Nitrogen saturation in northern forest ecosystems. Bioscience **39:** 378–386.

Alexander, R. B., A. H. Elliott, U. Shankar, and G. B. McBride. 2002. Estimating the sources and transport of nutrients in the Waikato River Basin, New Zealand. Water Resour. Res. **38:** 1268–1290.

———, R. A. Smith, and G. E. Schwartz. 2000. Effect of stream channel size on the delivery of nitrogen to the Gulf of Mexico. Nature **403:** 758–761.

Ashkenas, L. R., S. L. Johnson, S. V. Gregory, J. L. Tank, and W. M. Wollheim. 2004. A stable isotope tracer study of nitrogen uptake and transformation in an old-growth forest stream. Ecology **85:** 1725–1739.

Bernhardt, E. S., and others. 2005. Can't see the forest for the stream? In-stream processing and terrestrial nitrogen exports. BioScience **55:** 219–230.

Bernot, M. J., and W. K. Dodds. 2005. Nitrogen retention, removal, and saturation in lotic ecosystems. Ecosystems **8:** 442–453.

Burnham, K. R., and D. R. Anderson. 2002. Model selection and multimodel inference: A practical information theoretic approach, 2nd ed. Springer-Verlag.

Davis, J. C., and G. W. Minshall. 1999. Nitrogen and phosphorus uptake in two Idaho (USA) headwater wilderness streams. Oecologia **19:** 247–255.

Dodds, W. K., and others. 2002. N uptake as a function of concentration in streams. J. N. Am. Benthol. Soc. **21:** 206–220.

———, and E. B. Welch. 2000. Establishing nutrient criteria in streams. J. N. Am. Benthol. Soc. **19:** 186–196.

Earl, S. R., H. M. Valett, and J. R. Webster. 2006. Nitrogen saturation in stream ecosytems. Ecology **87:** 3140–3151.

Fellows, C. S., H. M. Valett, C. N. Dahm, P. J. Mulholland, and S. A. Thomas. 2006. Coupling nutrient uptake and energy flow in headwater streams. Ecosystems **9:** 788–804.

Fox, J. 2006. Structural equation modeling with the *sem* package in R. Struct. Eq. Model. **13:** 465–486.

Grace, J. B. 2006. Structural equation modeling in natural systems. Cambridge Univ. Press.

Gruber, N., and J. N. Galloway. 2008. An earth-system perspective of the global nitrogen cycle. Nature **451:** 293–296.

Hall, R. O., E. S. Bernhardt, and G. E. Likens. 2002. Linking nutrient uptake with transient storage in forested mountain streams. Limnol. Oceanogr. **47:** 255–265.

———, and J. L. Tank. 2003. Ecosystem metabolism controls nitrogen uptake in streams in Grand Teton National Park, Wyoming. Limnol. Oceanogr. **48:** 1120–1128.

Hedin, L. O., J. J. Armesto, and A. H. Johnson. 1995. Patterns of nutrient loss from unpolluted old-growth forests: Evaluation of biogeochemical theory. Ecology **76:** 493–509.

Hoellein, T. J., J. L. Tank, E. J. Rosi-Marshall, S. A. Entrekin, and G. A. Lamberti. 2007. Controls on spatial and temporal variation of nutrient uptake in three Michigan headwater streams. Limnol. Oceanogr. **52:** 1964–1977.

Howarth, R. W., and others. 1996. Regional nitrogen budgets and riverine N and P fluxes for the drainages to the North Atlantic Ocean: Natural and human influences. Biogeochemistry **35:** 75–139.

Kemp, W. M., and others. 2005. Eutrophication of Chesapeake Bay: Historical trends and ecological interactions. Mar. Ecol. Prog. Ser. **303:** 1–29.

Marzolf, E. R., P. J. Mulholland, and A. D. Steinman. 1994. Improvements to the diurnal upstream–downstream dissolved oxygen change technique for determining whole-stream metabolism in small streams. Can. J. Fish. Aquat. Sci. **51:** 1591–1599.

McClain, M. E., and others. 2003. Biogeochemical hot spots and hot moments at the interface of terrestrial and aquatic ecosystems. Ecosystems **6:** 301–312.

Mulholland, P. J., and others. 2009. Nitrate removal in stream ecosystems measured by ^{15}N addition experiments: Denitrification. Limnol. Oceanogr. **54:** 666–680.

———, and others. 2008. Stream denitrification across biomes and its response to anthropogenic nitrate loading. Nature **452:** 202–205.

———, and others. 2002. Can uptake length in streams be determined by nutrient addition experiments? Results from an inter-biome comparison study. J. N. Am. Benthol. Soc. **21:** 544–560.

———, S. A. Thomas, H. M. Valett, J. R. Webster, and J. Beaulieu. 2006. Effects of light on nitrate uptake in small forested streams: Diurnal and day-to-day variations. J. N. Am. Benthol. Soc. **25:** 583–595.

Newbold, J. D., and others. 2006. Uptake of nutrients and organic C in streams in New York City drinking-water supply watersheds. J. N. Am. Benthol. Soc. **25:** 998–1017.

———, J. W. Elwood, R. V. O'Neill, and W. Vanwinkle. 1981. Measuring nutrient spiraling in streams. Can. J. Fish. Aquat. Sci. **38:** 860–863.

———, S. A. Thomas, G. W. Minshall, C. E. Cushing, and T. Georgian. 2005. Deposition, benthic residence, and resuspension of fine organic particles in a mountain stream. Limnol. Oceanogr. **50:** 1571–1580.

O'Brien, J. M., W. K. Dodds, K. C. Wilson, J. N. Murdock, and J. Eichmiller. 2007. The saturation of N cycling in Central Plains streams: ^{15}N experiments across a broad gradient of nitrate concentrations. Biogeochemistry **84:** 31–49.

Odum, H. T. 1956. Primary production in flowing waters. Limnol. Oceanogr. **1:** 102–117.

Paul, M. J., and J. L. Meyer. 2001. Streams in the urban landscape. Ann. Rev. Ecol. Syst. **32:** 335–365.

Peterson, B. J., and others. 2001. Control of nitrogen export from watersheds by headwater streams. Science **292:** 86–90.

R Development Core Team. 2006. R: A language and environment for statistical computing. R Foundation for Statistical Computing, Vienna, Austria. ISBN 3-900051-07-0. Available from: http://www.R-project.org.

Rabalais, N. N., R. E. Turner, and W. J. Wiseman. 2002. Gulf of Mexico hypoxia, A.K.A the "dead zone". Ann. Rev. Ecol. Syst. **33:** 235–263.

Royer, T. V., M. B. David, and L. E. Gentry. 2006. Timing of riverine export of nitrate and phosphorus from agricultural watersheds in Illinois: Implications for reducing nutrient loading to the Mississippi River. Env. Sci. Tech. **40:** 4126–4131.

———, J. L. Tank, and M. B. David. 2004. Transport and fate of nitrate in headwater agricultural streams in Illinois. J. Env. Qual. **33:** 1296–1304.

Runkel, R. L. 1998. One-dimensional transport with inflow and storage (OTIS): A solute transport model for streams and rivers.U.S. Geological Survey, Water Resources Investigations Report 98-4018.

———. 2002. A new metric for determining the importance of transient storage. J. N. Am. Benthol. Soc. **21:** 529–543.

Schaefer, S. C., and M. Alber. 2007. Temperature controls a latitudinal gradient in the proportion of watershed nitrogen exported to coastal ecosystems. Biogeochemistry **85:** 333–346.

Seitzinger, S. P., and others. 2002. Nitrogen retention in rivers: Model development and application to watersheds in the northeastern U.S.A. Biogeochemistry **57:** 199–237.

Shipley, B. 2000. Cause and correlation in biology. Cambridge Univ. Press.

Sigman, D. M., and others. 1997. Natural abundance-level measurement of the nitrogen isotopic composition of oceanic nitrate: An adaptation of the ammonia diffusion method. Mar. Chem. **57:** 227–242.

Simon, K. S., C. R. Townsend, B. J. F. Biggs, and W. B. Bowden. 2005. Temporal variation of N and P uptake in 2 New Zealand streams. J. N. Am. Benthol. Soc. **24:** 1–18.

Stream Solute Workshop. 1990. Concepts and methods for assessing solute dynamics in stream ecosystems. J. N. Am. Benthol. Soc. **9:** 95–119.

Tank, J. L., E. J. Rosi-Marshall, M. A. Baker, and R. O. Hall. 2008. Are rivers just big streams? A pulse method to quantify nitrogen demand in a large river. Ecology **89:** 2935–2945.

Triska, F. J., V. C. Kennedy, R. J. Avanzino, G. W. Zellweger, and K. E. Bencala. 1989. Retention and transport of nutrients in a third order stream in northwest California: Hyporheic processes. Ecology **70:** 1893–1905.

Vannote, R. L., G. W. Minshall, K. W. Cummins, J. R. Sedell, and C. E. Cushing. 1980. The river continuum concept. Can. J. Fish. Aquat. Sci. **37:** 130–137.

Wanninkhof, R., P. J. Mulholland, and J. W. Elwood. 1990. Gas exchange rates for a first-order stream determined with deliberate and natural tracers. Water Resour. Res. **26:** 1621–1630.

Webster, J. R., and others. 2003. Factors affecting ammonium uptake in streams—an inter-biome perspective. Freshw. Biol. **48:** 1329–1352.

Wollheim, W. M., and others. 2001. Influence of stream size on ammonium and suspended particulate nitrogen processing. Limnol. Oceanogr. **46:** 1–13.

———, C. J. Vorösmarty, B. J. Peterson, S. P. Seitzinger, and C. S. Hopkinson. 2006. Relationship between river size and nutrient removal. Geophys. Res. Lett. **33:** LO6410, doi:10.1029/2006GL025845.

Associate editor: Samantha B. Joye

Received: 15 April 2008
Accepted: 29 September 2008
Amended: 15 October 2008